

On Tightly Bounding the Dubins Traveling Salesman's Optimum

Satyanarayana Manyam*, Sivakumar Rathinam†

Abstract

The Dubins Traveling Salesman Problem (DTSP) has generated significant interest over the last decade due to its occurrence in several civil and military surveillance applications. Currently, there is no algorithm that can find an optimal solution to the problem. In addition, relaxing the motion constraints and solving the resulting Euclidean TSP (ETSP) provides the only lower bound available for the problem. However, in many problem instances, the lower bound computed by solving the ETSP is far below the cost of the feasible solutions obtained by some well-known algorithms for the DTSP. This article addresses this fundamental issue and presents the first systematic procedure for developing tight lower bounds for the DTSP.

1. Introduction

Given a set of targets on a plane and a constant $\rho \geq 0$, the Dubins Traveling Salesman Problem (DTSP) aims to find a path such that each target is visited at least once, the radius of curvature of any point in the path is at least equal to ρ , and the length of the path is minimal. This problem is a generalization of the Euclidean TSP (ETSP) and is NP-hard [1, 2]. The DTSP belongs to a class of task allocation and path planning problems envisioned for a team of unmanned aerial vehicles in [3]. The DTSP has received significant attention in the literature [1, 2, 4–14], mainly due to its importance in unmanned vehicle applications, the simplicity of the problem statement, and its status as a hard problem to solve because it inherits features from both optimal control and combinatorial optimization.

Currently, there is no procedure for finding an optimal solution for the DTSP. Therefore, heuristics and approximation algorithms have been developed over the last decade to find feasible solutions. Tang and Ozguner [11] present gradient-based heuristics for both single and multiple vehicle variants of the DTSP. Savla et al. [12] use an optimal solution to the ETSP to find a feasible solution for the DTSP, and they bound the cost of the feasible solution with respect to the optimal cost of the ETSP. Rathinam et al. [1] develop an approximation algorithm for the DTSP in cases where the distance between any two targets is at least equal to 2ρ . Ny et al. [2] develop an approximation algorithm for the DTSP in which the approximation guarantee is inversely proportional to the minimum distance between any two targets. The weakness of the approximation guarantees of these algorithms for the DTSP is due to the lack of a good lower bound, as all these algorithms essentially use the Euclidean distances between the targets to bound the cost of a feasible solution.

Other heuristics have been used for solving the DTSP. A receding horizon approach that involves finding an optimal Dubins path through three consecutive targets is used to generate feasible solutions in [14]. The heuristic in [4] finds a feasible solution by minimizing the sum of the distances travelled by the vehicle and

*National Research Council Fellow, Air Force Research Laboratory, Dayton-Ohio, 45433.

†Associate Professor, Mechanical Engineering, Texas A & M University, College Station, TX-77843, **corresponding author:** srathinam@tamu.edu

the sum of the changes in the heading angles at each of the targets. Macharet et al. [5, 7] first obtain a tour by solving the ETSP and then select the heading angle at each target using an orientation-assignment heuristic. A multiple lookahead approach is used to find feasible solutions in [8, 15]. Meta-heuristics have also been developed to find feasible solutions for the DTSP in [9, 10].

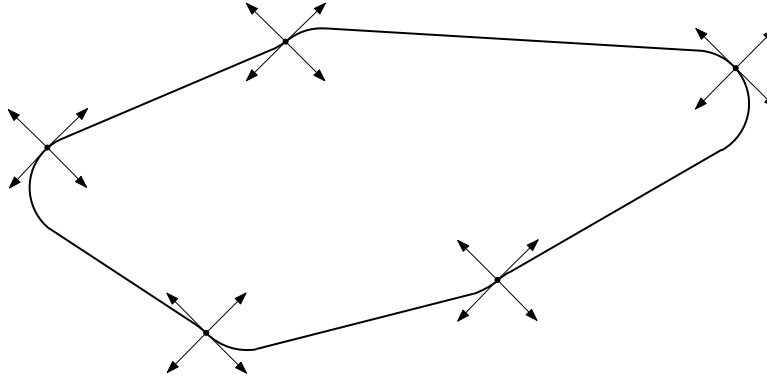


Figure 1. There are four possible headings at each target. A feasible solution for the DTSP can be obtained by choosing a heading at each target and finding a corresponding optimal TSP path.

Another common approach [13, 16] involves discretizing the heading angle at each target and posing the resulting problem as a one-in-a-set TSP (Fig. 1). The greater the number of discretizations, the closer an optimal one-in-a-set TSP solution gets to the optimal DTSP solution. This approach provides a natural way to find a good, feasible solution to the problem [16]. However, this also requires us to solve a large one-in-a-set TSP, which is combinatorially hard. Nevertheless, this approach provides an upper bound [13] for the optimal cost of the DTSP, and simulation results indicate that the cost of the solutions start to converge with more than 15 discretizations at each target.

The fundamental question with regard to all the above heuristics and approximation algorithms is how close a feasible solution *actually is* to the optimum. For example, Fig. 2 shows the cost of the feasible solutions obtained by solving the one-in-a-set TSP and the ETSP for 25 instances with 20 targets in each instance. Even with 32 discretizations of the possible angles at each target, the cost of the feasible solution is at least 30% greater than the corresponding optimal ETSP cost for several of these instances. As the optimal cost is not known for the DTSP, identifying a tight lower bound is crucial for determining the quality of the solutions that have been provided as well as for developing constant factor approximation algorithms.

This fundamental question was the motivation for the bounding algorithms in [17–20]. In these algorithms, the requirement that the arrival and departure angles must be equal at each target is removed, and instead there is a penalty in the objective function whenever the requirement is violated. This results in a max-min problem where the minimization problem is an asymmetric TSP (ATSP) and the cost of traveling between any two targets requires solving a new optimal control problem. In terms of lower bounding, the difficulty with this approach is that we are not currently aware of any algorithm that will guarantee a lower bound for the optimal control problem. Nonetheless, this is a useful approach, and advances in lower bounding optimal control problems will lead to finding lower bounds for the DTSP.

In this article, we propose a new approach to finding tight lower bounds for the DTSP. This is the first systematic procedure available for the DTSP and is a natural counterpart to the one-in-a-set TSP approach we discussed above. In this approach, we remove the requirement that the arrival angle and the departure angle at each target must be the same, but we restrain these angles so that they belong to one sector or interval (refer to Fig. 3). The lower bounding problem aims to choose an interval at each target such that the arrival angle and the departure angle at the target belong to the same interval, each target is visited at

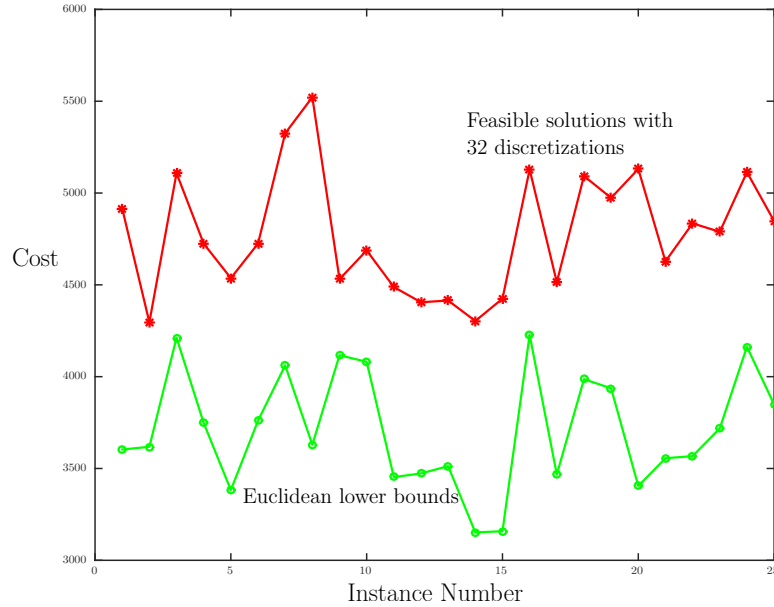


Figure 2. A comparison between the cost of the feasible solution (upper bound) obtained by solving the one-in-a-set TSP with 32 discretizations and the optimal cost of the corresponding Euclidean TSP (lower bound) for 25 instances. There are 20 targets in each instance, and the location of each target is sampled from a 1000×1000 square. Also, the minimum turning radius of the vehicle is set to 100.

least once, and the sum of the costs of travelling between the targets is minimized. The cost of traveling between two intervals corresponding to two distinct targets now reduces to a new optimal control problem, which we refer to as the **Dubins interval problem**. Given two targets and an interval at each target, the problem is to find a Dubins path such that the departure angle at the initial target and the arrival angle at the final target belong to the given intervals and the length of the path is minimal. The lower bounding problem is a one-in-a-set TSP and can be solved just like the upper bounding problem. If the size of each of the intervals at each target reduces to zero, the lower bounding problem reduces to the DTSP. If there is only one interval of size 2π at each target, the result is a Euclidean TSP. As the size of the intervals at the targets becomes smaller, the one-in-a-set TSP becomes combinatorially hard, similar to the upper bounding problem. Nevertheless, this provides a systematic approach to finding lower bounds for the DTSP, provided the Dubins interval problem can be solved.

The Dubins interval problem is a new generalization of the standard Dubins problem [25] which has not been formulated or solved¹ in the literature. The difficulty with solving this problem lies in the fact that the length of the shortest Dubins paths between any two targets is a non-linear, discontinuous function of the heading angles of the targets. Therefore, finding the optimal heading angles from the given intervals at the targets that minimizes the length of the Dubins path is non-trivial. In this article, we solve the Dubins interval problem using the monotonicity properties and the extremal values of the length of the Dubins paths.

The following are the contributions of this article:

¹We point out that we are also working on a completely different approach which is based on optimal control in [21]. However, the approach in [21] still relies on the results of this paper. Second, unlike the analysis and results in this paper, the work in [21] does not provide information about the rate of change of lengths of the Dubins paths as a function of the heading angles at the targets. This information is critical and very useful in the development of bounds for feasible solutions and approximation algorithms for the DTSP.

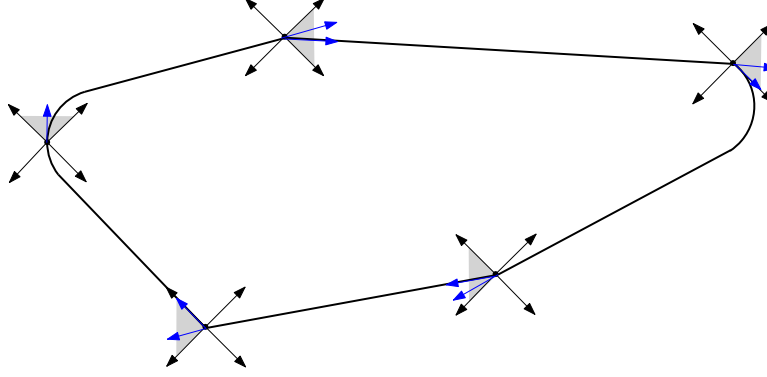


Figure 3. There are four intervals at each target. A lower bound for the DTSP can be obtained by choosing an interval and restricting both the arrival and the departure angles to be in the chosen interval at each target, and then finding a corresponding optimal TSP path. The shaded interval at each target shows the chosen interval with the arrival and departure angles in blue.

1. The formulation of the lower bounding problem for the DTSP as a novel one-in-a-set TSP where the cost of traveling between any two targets requires solving a Dubins Interval Problem. This is the first formulation that aims to provide a tight lower bound for the DTSP.
2. The first algorithm to solve the Dubins Interval Problem by exploiting its structure and monotonicity properties.
3. Numerical results to corroborate the performance of the proposed lower bounding approach for the 25 instances shown in figure 2.

2. Lower Bounding Problem Formulation

The set of targets is denoted by $T = \{1, 2, \dots, n\}$, where n is the number of targets. The set of available angles $[0, 2\pi]$ at any target i is partitioned into a collection of closed intervals denoted by $\mathcal{S}_i := \{[0, \varphi_{i1}], [\varphi_{i1}, \varphi_{i2}], \dots, [\varphi_{im_i-1}, \varphi_{im_i} = 2\pi]\}$, where $m_i (\geq 1)$ denotes the number of intervals at target i and the φ_{ij} are constants such that $0 \leq \varphi_{i1} \leq \varphi_{i2} \leq \dots \leq \varphi_{im_i} = 2\pi$. Let (x_i, y_i) denote the location of target $i \in T$, and let the arrival angle and the departure angle of the vehicle at target i be denoted by θ_{ia} and θ_{id} , respectively. The configuration of the vehicle leaving target i at θ_{id} is then denoted by (x_i, y_i, θ_{id}) , and (x_i, y_i, θ_{ia}) similarly denotes the vehicle's arrival configuration. The length of the shortest Dubins path from (x_i, y_i, θ_{id}) to (x_j, y_j, θ_{ja}) is denoted by $d_{ij}(\theta_{id}, \theta_{ja})$. Given an interval I_i at target i and an interval I_j at target j , define $d_{ij}^*(I_i, I_j) := \min_{\theta_{id} \in I_i, \theta_{ja} \in I_j} d_{ij}(\theta_{id}, \theta_{ja})$. The objective of the Bounding Problem (**BP**) is to find a sequence of targets (s_1, s_2, \dots, s_n) , $s_i \in T$, to visit and an interval $I_{s_i} \in \mathcal{S}_{s_i}$ for each target $s_i \in T$ such that

- each target is visited at least once, and
- the cost $\sum_{i=1}^{n-1} d_{s_i s_{i+1}}^*(I_{s_i}, I_{s_{i+1}}) + d_{s_n s_1}^*(I_{s_n}, I_{s_1})$ is minimized.

Addressing this **BP** first requires solving $\min_{\theta_{id} \in I_i, \theta_{ja} \in I_j} d_{ij}(\theta_{id}, \theta_{ja})$. Once this problem is solved, the **BP** is essentially a one-in-a-set TSP. In this article, we transform the one-in-a-set TSP into an ATSP using the Noon-Bean transformation [22] and then convert the resulting ATSP into a symmetric TSP using the transformation in [23]. The symmetric TSP is solved using the Concorde solver [24] to find an optimal solution.

Prior to addressing the Dubins Interval Problem in the next section, we first formally state the lower bounding result in the following proposition.

Proposition 2.1. *The optimal cost to the **BP** is a lower bound to the DTSP.*

Proof. Any optimal solution to the DTSP is a feasible solution to the **BP** for any positive number of intervals at each target. Therefore, the optimal cost of the **BP** must be a lower bound to the optimal cost of the DTSP. \square

3. Dubins Interval Problem

Without loss of generality, let the Dubins interval problem be denoted as $\min_{\theta_1 \in I_1, \theta_2 \in I_2} d_{12}(\theta_1, \theta_2)$, where $d_{12}(\theta_1, \theta_2)$ indicates the shortest path (also referred to as the Dubins path) for traveling from (x_1, y_1, θ_1) to (x_2, y_2, θ_2) subject to the minimum turning radius constraint (Fig. 4). Here the interval I_k is defined as $[\theta_k^{\min}, \theta_k^{\max}] \subseteq [0, 2\pi]$ for $k = 1, 2$. Given an initial configuration (x_1, y_1, θ_1) and a final configuration (x_2, y_2, θ_2) , L.E. Dubins [25] showed that the shortest path for a vehicle to travel between the two configurations subject to the minimum turning radius (ρ) constraint must consist of at most three segments, where each segment is a circle of radius ρ or a straight line. Specifically, if a curved segment of radius ρ along which the vehicle travels in a counterclockwise (clockwise) rotational motion is denoted by $L(R)$, and the segment along which the vehicle travels straight is denoted by S , then the shortest path is one of RSR , RSL , LSR , LSL , RLR , and LRL .

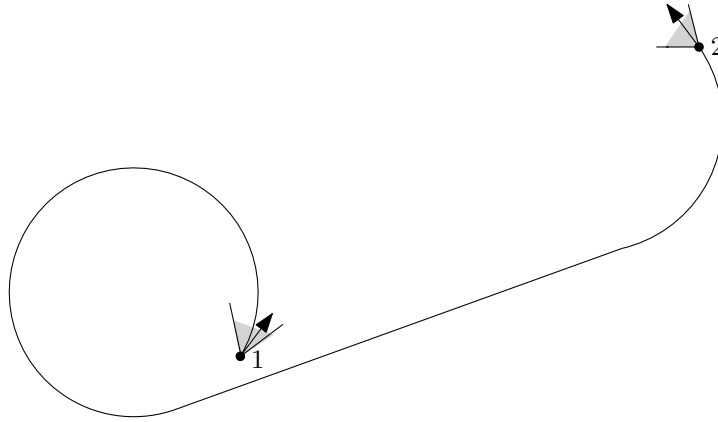


Figure 4. A feasible solution to the Dubins interval problem.

Let $RSL(\theta_1, \theta_2)$ denote the length of the RSL path from (x_1, y_1, θ_1) to (x_2, y_2, θ_2) . $RSL(\theta_1, \theta_2)$ is set to ∞ if the RSL path does not exist. Let $RSR(\theta_1, \theta_2)$, $LSR(\theta_1, \theta_2)$, $LSL(\theta_1, \theta_2)$, $RLR(\theta_1, \theta_2)$, and $LRL(\theta_1, \theta_2)$ be defined in a similar way. Using these definitions, the Dubins interval problem can be written as follows:

$$\min_{\theta_1 \in I_1, \theta_2 \in I_2} d_{12}(\theta_1, \theta_2) = \min_{\theta_1 \in I_1, \theta_2 \in I_2} \{RSR(\theta_1, \theta_2), RSL(\theta_1, \theta_2), LSR(\theta_1, \theta_2), LSL(\theta_1, \theta_2), RLR(\theta_1, \theta_2), LRL(\theta_1, \theta_2)\}. \quad (1)$$

Remark 3.1. $d_{12}(\theta_1, \theta_2)$ is a lower semicontinuous function and is minimized over closed and bounded intervals I_1 and I_2 . Therefore, the Dubins interval problem is well defined, i.e., there exist $\theta_1^* \in I_1$ and $\theta_2^* \in I_2$ such that $d_{12}(\theta_1^*, \theta_2^*) = \min_{\theta_1 \in I_1, \theta_2 \in I_2} d_{12}(\theta_1, \theta_2)$.

To solve the Dubins interval problem, we also consider shortest paths that contain at most two segments between (x_1, y_1) and (x_2, y_2) . For any path $\mathcal{T} \in \{RS, LS, SR, SL, RL, LR\}$ and $\theta_1 \in I_1$, let $\mathcal{T}^1(\theta_1)$ denote the distance of the shortest path of type \mathcal{T} that starts at (x_1, y_1) with a departure angle of θ_1 and arrives at

(x_2, y_2) with an arrival angle in I_2 . In this case, the arrival angle at (x_2, y_2) will be a function of θ_1 and \mathcal{T} and is denoted as $\theta_2(\mathcal{T}, \theta_1)$. $\mathcal{T}^1(\theta_1)$ is set to ∞ if a path of type \mathcal{T} does not exist or if $\theta_2(\mathcal{T}, \theta_1) \notin I_2$. Similarly, let $\mathcal{T}^2(\theta_2)$ denote the distance of the shortest path of type \mathcal{T} that starts at (x_1, y_1) with a departure angle in I_1 and arrives at (x_2, y_2) with an arrival angle of θ_2 . In this case, the departure angle at (x_1, y_1) will be a function of θ_2 and \mathcal{T} and is denoted as $\theta_1(\mathcal{T}, \theta_2)$. $\mathcal{T}^2(\theta_2)$ is set to ∞ if the path of type \mathcal{T} does not exist or if $\theta_1(\mathcal{T}, \theta_2) \notin I_1$. From the definitions, note that $\min_{\theta_1 \in I_1} \mathcal{T}^1(\theta_1) = \min_{\theta_2 \in I_2} \mathcal{T}^2(\theta_2)$.

The following theorem provides a way to further simplify equation (1) and solve the Dubins interval problem:

Theorem 3.1.

$$\min_{\theta_1 \in I_1} \min_{\theta_2 \in I_2} \{d_{12}(\theta_1, \theta_2)\} = \min\{d^*, \min_{\theta_1 \in I_1} \{RS^1(\theta_1), SR^1(\theta_1), LS^1(\theta_1), SL^1(\theta_1), LR^1(\theta_1), RL^1(\theta_1)\}\} \quad (2)$$

where

$$d^* := \min\{d_{12}(\theta_1^{min}, \theta_2^{min}), d_{12}(\theta_1^{max}, \theta_2^{min}), d_{12}(\theta_1^{min}, \theta_2^{max}), d_{12}(\theta_1^{max}, \theta_2^{max})\}.$$

In English, this theorem states that an optimal path to the Dubins interval problem must be one of the following:

1. An optimal Dubins path consisting of at most three segments such that both the arrival and departure angles at each target belong to one of the boundary values of the respective intervals, or
2. An optimal Dubins path consisting of at most two segments such that the angle constraints are satisfied.

After proving this theorem in the next subsection, we will provide algorithms to solve for the optimal Dubins paths with at most two segments (i.e., to solve $\min_{\theta_1 \in I_1} \mathcal{P}(\theta_1)$ for any path $\mathcal{P} \in \{RS^1, SR^1, LS^1, SL^1, LR^1, RL^1\}$). As d^* in the above theorem can already be computed directly using Dubins's result [25], one can then compute the optimal cost for the Dubins interval problem and the corresponding departure and arrival angles.

3.1. Proof of Theorem 3.1

This theorem will be proved in two parts. First, we will first show how to simplify $\min_{\theta_1 \in I_1, \theta_2 \in I_2} \mathcal{P}(\theta_1, \theta_2)$ for any path $\mathcal{P} \in \{RSR, RSL, LSR, LSL\}$. Then we will address the *LRL* and the *RLR* paths.

3.1.1. Optimizing RSR, RSL, LSR, and LSL paths. The following result is known [26] for each of the paths $\mathcal{P} \in \{RSR, RSL, LSR, LSL\}$ from (x_1, y_1, θ_1) to (x_2, y_2, θ_2) :

Lemma 3.1. *For any $\mathcal{P} \in \{RSR, RSL, LSR, LSL\}$ and $i = 1, 2$, either $\frac{\partial \mathcal{P}(\theta_1, \theta_2)}{\partial \theta_i} \geq 0 \forall \theta_i$ or $\frac{\partial \mathcal{P}(\theta_1, \theta_2)}{\partial \theta_i} \leq 0 \forall \theta_i$ when \mathcal{P} exists and none of its curved segments vanish.*

Now let us apply the above lemma to the *RSL* path. The *RSL* path ceases to exist when the segment *S* vanishes, i.e., the *RSL* path reduces to an *RL* path. In addition, when one of the curved segments vanishes, the *RSL* path reduces to either the *RS* or the *SL* path (refer to Fig. 5). Therefore, given θ_1 , the optimum for $\min_{\theta_2 \in [\theta_2^{min}, \theta_2^{max}]} RSL(\theta_1, \theta_2)$ must be attained when $\theta_2 = \theta_2^{min}$ or $\theta_2 = \theta_2^{max}$ or when the *RSL* path reduces to an *RL*, *RS*, or *SL* path. This can be stated as follows:

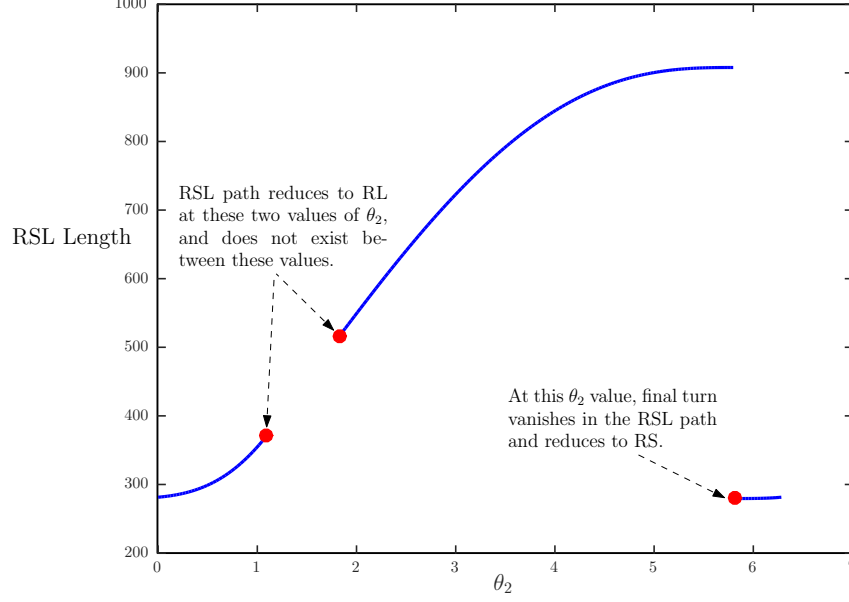


Figure 5. Given θ_1 , the length of the RSL path varies monotonically with respect to θ_2 wherever the path exists and none of its curved segments vanish.

$$\min_{\theta_2 \in I_2} \{RSL(\theta_1, \theta_2)\} := \min\{RSL(\theta_1, \theta_2^{min}), RSL(\theta_1, \theta_2^{max}), RS^1(\theta_1), SL^1(\theta_1), RL^1(\theta_1)\}. \quad (3)$$

Therefore,

$$\begin{aligned} & \min_{\theta_1 \in I_1} \min_{\theta_2 \in I_2} \{RSL(\theta_1, \theta_2)\} \\ &= \min_{\theta_1 \in I_1} \min\{RSL(\theta_1, \theta_2^{min}), RSL(\theta_1, \theta_2^{max}), RS^1(\theta_1), SL^1(\theta_1), RL^1(\theta_1)\} \\ &= \min\{\min_{\theta_1 \in I_1} RSL(\theta_1, \theta_2^{min}), \min_{\theta_1 \in I_1} RSL(\theta_1, \theta_2^{max}), \min_{\theta_1 \in I_1} \{RS^1(\theta_1), SL^1(\theta_1), RL^1(\theta_1)\}\}. \end{aligned} \quad (4)$$

Similarly, using Lemma 3.1 again, we get the following:

$$\min_{\theta_1 \in I_1} RSL(\theta_1, \theta_2^{min}) = \min\{RSL(\theta_1^{min}, \theta_2^{min}), RSL(\theta_1^{max}, \theta_2^{min}), RS^2(\theta_2^{min}), SL^2(\theta_2^{min}), RL^2(\theta_2^{min})\}, \quad (5)$$

$$\min_{\theta_1 \in I_1} RSL(\theta_1, \theta_2^{max}) = \min\{RSL(\theta_1^{min}, \theta_2^{max}), RSL(\theta_1^{max}, \theta_2^{max}), RS^2(\theta_2^{max}), SL^2(\theta_2^{max}), RL^2(\theta_2^{max})\}. \quad (6)$$

Now, one can easily verify the following:

$$\text{For any } \mathcal{T} \in \{RS, SL, RL\}, \quad \min_{\theta_1 \in I_1} \mathcal{T}^1(\theta_1) \leq \mathcal{T}^2(\theta_2^{min}) \text{ and } \min_{\theta_1 \in I_1} \mathcal{T}^1(\theta_1) \leq \mathcal{T}^2(\theta_2^{max}). \quad (7)$$

Substituting for $\min_{\theta_1 \in I_1} RSL(\theta_1, \theta_2^{min})$ and $\min_{\theta_1 \in I_1} RSL(\theta_1, \theta_2^{max})$ in (4) using equations (5) and (6) and simplifying further using (7), we get

$$\min_{\theta_1 \in I_1} \min_{\theta_2 \in I_2} RSL(\theta_1, \theta_2) = \min\{RSL^*, \min_{\theta_1 \in I_1} \{RS^1(\theta_1), SL^1(\theta_1), RL^1(\theta_1)\}\}, \quad (8)$$

where

$$RSL^* := \min\{RSL(\theta_1^{min}, \theta_2^{min}), RSL(\theta_1^{max}, \theta_2^{min}), RSL(\theta_1^{min}, \theta_2^{max}), RSL(\theta_1^{max}, \theta_2^{max})\}.$$

As Lemma 3.1 is also applicable to RSR , LSL , and LSR paths, one can use the above procedure and simplify $\min_{\theta_1 \in I_1, \theta_2 \in I_2} RSR(\theta_1, \theta_2)$, $\min_{\theta_1 \in I_1, \theta_2 \in I_2} LSL(\theta_1, \theta_2)$, and $\min_{\theta_1 \in I_1, \theta_2 \in I_2} LSR(\theta_1, \theta_2)$ in a similar way. Combining all these results, we obtain the following:

$$\min_{\theta_1 \in I_1} \min_{\theta_2 \in I_2} \min_{\mathcal{P} \in \{RSR, RSL, LSR, LSL\}} \mathcal{P}(\theta_1, \theta_2) = \min\{\mathcal{P}^*, \min_{\theta_1 \in I_1} \{RS^1(\theta_1), SR^1(\theta_1), LS^1(\theta_1), SL^1(\theta_1), LR^1(\theta_1), RL^1(\theta_1)\}\} \quad (9)$$

where

$$\mathcal{P}^* := \min_{\mathcal{P} \in \{RSR, RSL, LSR, LSL\}} \min\{\mathcal{P}(\theta_1^{min}, \theta_2^{min}), \mathcal{P}(\theta_1^{max}, \theta_2^{min}), \mathcal{P}(\theta_1^{min}, \theta_2^{max}), \mathcal{P}(\theta_1^{max}, \theta_2^{max})\}.$$

3.1.2. Optimizing RLR and LRL paths. Xavier et al. [26] have shown that the RLR and LRL paths cannot lead to an optimal Dubins path if the distance between the two targets is greater than 4ρ . Therefore, in this section, we assume that the distance between the two targets is at most 4ρ . We will focus on $\min_{\theta_1 \in I_1, \theta_2 \in I_2} LRL(\theta_1, \theta_2)$; $\min_{\theta_1 \in I_1, \theta_2 \in I_2} RLR(\theta_1, \theta_2)$ can be solved in a similar way. Given θ_1 , unlike the length of the RSL path, $LRL(\theta_1, \theta_2)$ is not monotonous with respect to θ_2 when LRL exists. Without loss of generality, we assume that $\theta_1 = 0$ and first aim to understand $LRL(0, \theta_2)$ as a function of θ_2 (refer to Fig. 6). Target 1 is located at the origin and target 2 is located at (\bar{x}, \bar{y}) . The angles α and β in Fig. 6 are functions of θ_2 . For brevity, we use α and β in place of $\alpha(\theta_2)$ and $\beta(\theta_2)$, respectively. Let $LRL(0, \theta_2)$ be denoted as $\mathfrak{D}(\theta_2) := (2\pi + 2\alpha + 2\beta + \theta_2)\rho$. In the ensuing discussion, we use the fact that the length of the R segment in an LRL path must be greater than $\pi\rho$ (i.e., $0 < \alpha + \beta < \pi$) for the LRL path to be an optimal Dubins path between any two targets [25, 27].

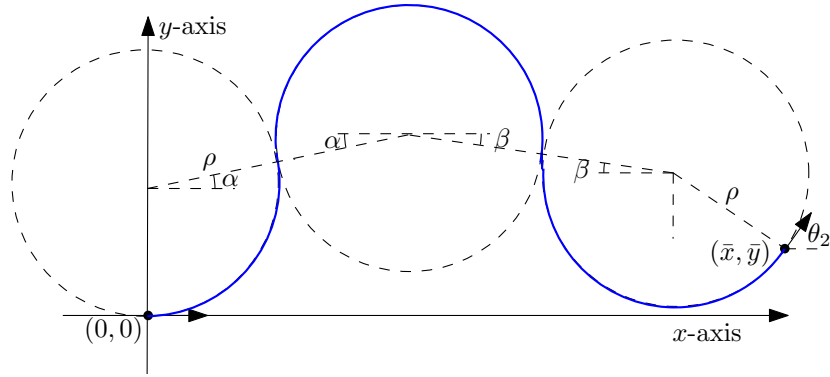


Figure 6. LRL path for $\theta_1 = 0$.

Lemma 3.2. *If the LRL path exists and none of its curved segments vanish, then for any θ_2 such that $0 < \alpha(\theta_2) + \beta(\theta_2) < \pi$, $\frac{\partial \mathfrak{D}}{\partial \theta_2} \neq 0$ except when $\mathfrak{D}(\theta_2)$ reaches a maximum, when θ_2 satisfies $\alpha + \pi/2 = \theta_2$.*

Proof. Using Fig. 6, α and β can be obtained in terms of θ_2 as follows:

$$2\rho \sin \alpha + \rho = 2\rho \sin \beta + \rho \cos \theta_2 + \bar{y}, \quad (10)$$

$$2\rho \cos \alpha + 2\rho \cos \beta + \rho \sin \theta_2 = \bar{x}. \quad (11)$$

Differentiating and simplifying the above equations, we get

$$\cos \alpha \frac{d\alpha}{d\theta_2} - \cos \beta \frac{d\beta}{d\theta_2} = -\frac{\sin \theta_2}{2}, \quad (12)$$

$$\sin \alpha \frac{d\alpha}{d\theta_2} + \sin \beta \frac{d\beta}{d\theta_2} = \frac{\cos \theta_2}{2}. \quad (13)$$

Further solving for the derivatives, we get

$$\frac{d\beta}{d\theta_2} = \frac{\cos(\theta_2 - \alpha)}{2\sin(\alpha + \beta)}, \quad (14)$$

$$\frac{d\alpha}{d\theta_2} = \frac{\cos(\theta_2 + \beta)}{2\sin(\alpha + \beta)}. \quad (15)$$

Therefore,

$$\frac{d\mathcal{D}}{d\theta_2} = \rho \left(2 \frac{d\beta}{d\theta_2} + 2 \frac{d\alpha}{d\theta_2} + 1 \right) \quad (16)$$

$$= \rho \left(\frac{\cos(\theta_2 - \alpha)}{\sin(\alpha + \beta)} + \frac{\cos(\theta_2 + \beta)}{\sin(\alpha + \beta)} + 1 \right). \quad (17)$$

Equation $\frac{d\mathcal{D}}{d\theta_2} = 0$ yields the following possibilities: $\theta_2 = \frac{\pi}{2} + \alpha$ or $\theta_2 + \beta = -\frac{\pi}{2}$. $\theta_2 + \beta = -\frac{\pi}{2}$ corresponds to the case where the second left turn disappears; there is a jump in the length of the *LRL* path at this θ_2 , and therefore $\frac{d\mathcal{D}}{d\theta_2}$ does not exist. $\theta_2 = \frac{\pi}{2} + \alpha$ corresponds to the case where the turn angle in the right turn is equal to the turn angle in the second left turn; one can verify that $\mathcal{D}(\theta_2)$ reaches a maximum at this point because $\frac{d^2\mathcal{D}}{d\theta_2^2} = -\frac{3\rho}{2} \frac{1+\cos(\alpha+\beta)}{\sin(\alpha+\beta)} < 0$ (refer to Fig. 7). □

The derivatives of $LRL(\theta_1, \theta_2)$ do not exist when any turn in the path disappears or when the angle in the right turn becomes equal to π , as shown in Fig. 8. The length of the two paths (Fig. 8) when the *LRL* path just ceases to exist are denoted by $LRL_a^1(\theta_1)$ and $LRL_b^1(\theta_1)$. Therefore, applying the above lemma to the *LRL* path and following similar steps to those in subsection 3.1.1, we get the following result:

$$\min_{\theta_2 \in I_2} \{LRL(\theta_1, \theta_2)\} := \min\{LRL(\theta_1, \theta_2^{min}), LRL(\theta_1, \theta_2^{max}), LR^1(\theta_1), RL^1(\theta_1), LRL_a^1(\theta_1), LRL_b^1(\theta_1)\}. \quad (18)$$

Again, as in subsection 3.1.1, one can further simplify the above optimization problem:

$$\min_{\theta_1 \in I_1} \min_{\theta_2 \in I_2} \{LRL(\theta_1, \theta_2)\} = \min\{LRL^*, \min_{\theta_1 \in I_1} \{LR^1(\theta_1), RL^1(\theta_1), LRL_a^1(\theta_1), LRL_b^1(\theta_1)\}\} \quad (19)$$

where

$$LRL^* := \min\{LRL(\theta_1^{min}, \theta_2^{min}), LRL(\theta_1^{max}, \theta_2^{min}), LRL(\theta_1^{min}, \theta_2^{max}), LRL(\theta_1^{max}, \theta_2^{max})\}.$$

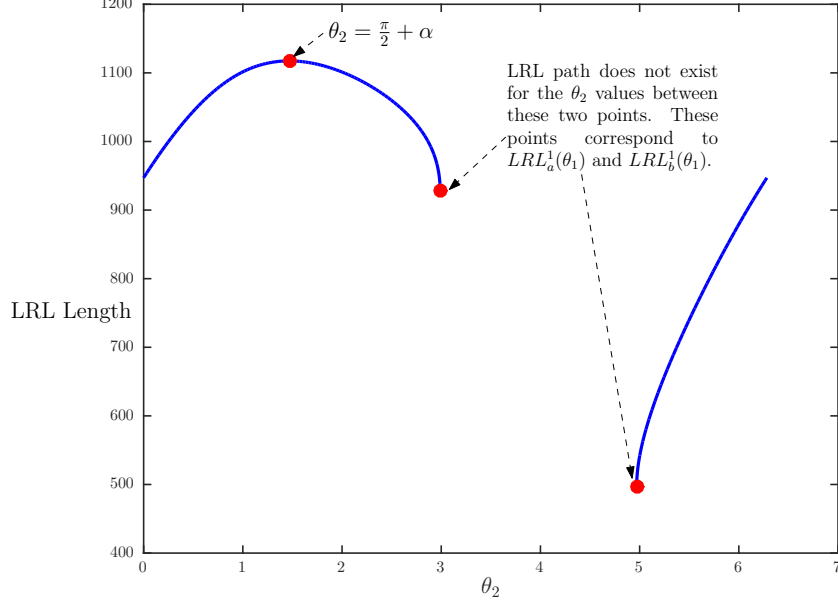


Figure 7. Given θ_1 , the length of the *LRL* path reaches a maximum when $\theta_2 = \frac{\pi}{2} + \alpha$, as shown. This figure also shows the values of θ_2 where the *LRL* path just ceases to exist.

Note that $LRL_a^1(\theta_1)$ and $LRL_b^1(\theta_1)$ can never result in an optimal Dubins path because the angle in the right turn is equal to π [27]. Therefore, once equation (19) is substituted in equation (1), the functions $LRL_a^1(\theta_1)$ and $LRL_b^1(\theta_1)$ will drop out.

$\min_{\theta_1 \in I_1} \min_{\theta_2 \in I_2} \{RLR(\theta_1, \theta_2)\}$ can be simplified in a similar way. Hence, combining the above results with equation (9), we obtain the result stated in Theorem 3.1.

4. Algorithms for Optimizing Dubins Paths with At Most Two Segments

The only remaining step needed to solve the Dubins interval problem is to show how to optimize $\min_{\theta_1 \in I_1} \{RS^1(\theta_1), SR^1(\theta_1), LS^1(\theta_1), SL^1(\theta_1), LR^1(\theta_1), RL^1(\theta_1)\}$. In this section, we will solve two problems: $\min_{\theta_1 \in I_1} \{RS^1(\theta_1)\}$ and $\min_{\theta_1 \in I_1} \{RL^1(\theta_1)\}$. The remaining paths can be solved using simple transformations (reflections about the x or the y axis).

4.1. Optimizing the RS path

Without loss of generality, a reference frame can be chosen such that target 1 is at the origin and target 2 lies on the x -axis as shown in Fig. 9. Here \bar{x} represents the Euclidean distance between the targets. Given θ_1 , the existence of the *RS* path as well as its length can be determined using geometry. The length of the *S* path, the angle between the x -axis and the *S* path, and the final arrival angle at target 2 are also functions of θ_1 and can be expressed as $L(\theta_1)$, $\phi(\theta_1)$, and $\theta_2(RS, \theta_1)$, respectively. Let the length of the *RS* path be denoted as $\mathcal{D}(\theta_1)$. For brevity, in some places we will use L , ϕ , θ_2 , and \mathcal{D} instead of $L(\theta_1)$, $\phi(\theta_1)$, $\theta_2(RS, \theta_1)$, and $\mathcal{D}(\theta_1)$, respectively. Let $d_S := \bar{x}$ if the angle of the straight line joining the two targets lies in the intervals I_1 and I_2 . If the angle constraints are not satisfied, d_S is set to ∞ . Similarly, let d_R denote the length of the shortest circular arc of type *R* that joins the two targets such that the boundary angles of the arc belong to the respective intervals at the targets. If such an arc does not exist, d_R is set to ∞ . In the following lemma, we assume that $[\theta_1^{min}, \theta_1^{max}] \subseteq [0, 2\pi]$ and $[\theta_2^{min}, \theta_2^{max}] \subseteq [0, 2\pi]$.

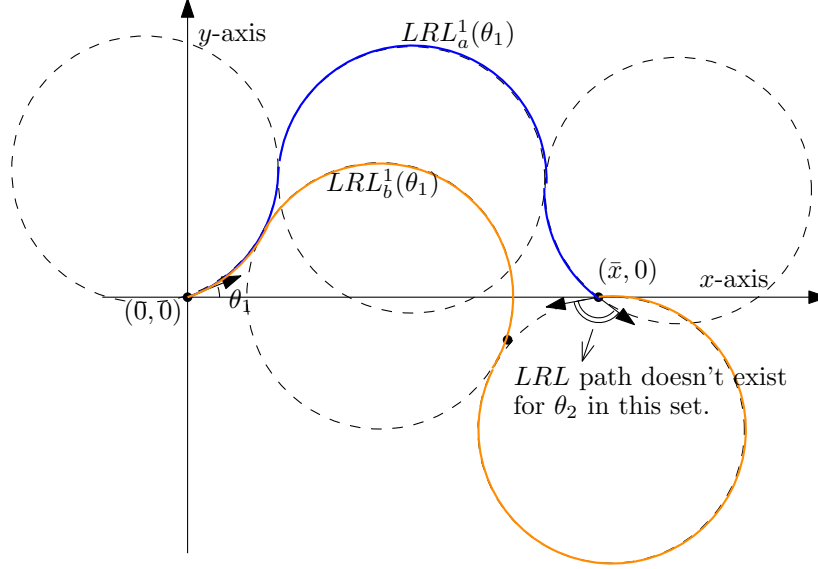


Figure 8. Given θ_1 , the LRL paths when the arc angle in the right turn is π . This figure shows the angles for θ_2 when the LRL path does not exist.

Lemma 4.1. $\min_{\theta_1 \in I_1} \{RS^1(\theta_1)\} := \min\{d_S, d_R, RS^1(\theta_1^{min}), RS^2(\theta_2^{min}), RS^2(\theta_2^{max})\}$.

Proof. Refer to the appendix for the proof. □

4.2. Optimizing the RL path

We use similar notations as in previous subsections (refer to Fig. 10). The angles $\phi(\theta_1)$ and $\theta_2(RL, \theta_1)$ are also written as ϕ and θ_2 , for brevity. The length of the RL path is denoted as $\mathcal{D}(\theta_1)$ and is equal to $\rho(\theta_1 + \theta_2 + 2\phi)$. RL paths do not exist when $\bar{x} > 4\rho$. In addition, even when $0 \leq \bar{x} \leq 4\rho$, there are a subset of angles of θ_1 for which an RL path does not exist. Moreover, given θ_1 , there are two possible RL paths, as either $\phi + \theta_2 \leq \pi$ or $\phi + \theta_2 > \pi$. In the following discussion and in Fig. 10, we assume that $\phi + \theta_2 < \pi$. The other RL path can be addressed similarly.

We first define some values of θ_1 where the optimum can occur (these correspond to the extreme values of \mathcal{D} and θ_2 for the RL path and will be derived later in the proof). Let θ^{1*} be the solution to the equation $\theta_2(RL, \theta_1) = \theta_1$. Also, let θ^{2*} and θ^{3*} be the solutions to equation $\phi(\theta_1) + \theta_2(RL, \theta_1) = \pi$. Let d_L denote the length of the shortest circular arc of type L that joins the two targets such that the boundary angles of the arc belong to the corresponding intervals at the targets and $\phi + \theta_2 < \pi$. If such an arc does not exist, then d_L is set to ∞ . Let $RL^* = \min\{RL^1(\theta_1^{max}), RL^1(\theta_1^{min}), RL^2(\theta_2^{min}), RL^2(\theta_2^{max})\}$.

Lemma 4.2. If $\bar{x} > 2\rho$, $\min_{\theta_1 \in I_1} \{RL^1(\theta_1)\} := \min\{RL^1(\theta^{1*}), RL^1(\theta^{2*}), RL^1(\theta^{3*}), RL^*\}$. If $0 \leq \bar{x} \leq 2\rho$, $\min_{\theta_1 \in I_1} \{RL^1(\theta_1)\} := \min\{d_L, d_R, RL^1(\theta^{1*}), RL^*\}$.

Proof. Refer to the appendix. □

5. Numerical results

Computational results are presented for 25 instances with 20 targets in each instance. The locations of the targets were sampled from a 1000×1000 square. The minimum turning radius of the vehicle was chosen to be 100. The heading angles at each target are discretized into 4, 8, 16, and 32 intervals. We use the Noon-Bean transformation to first convert the one-in-a-set TSP into an ATSP. Then we use a transformation method

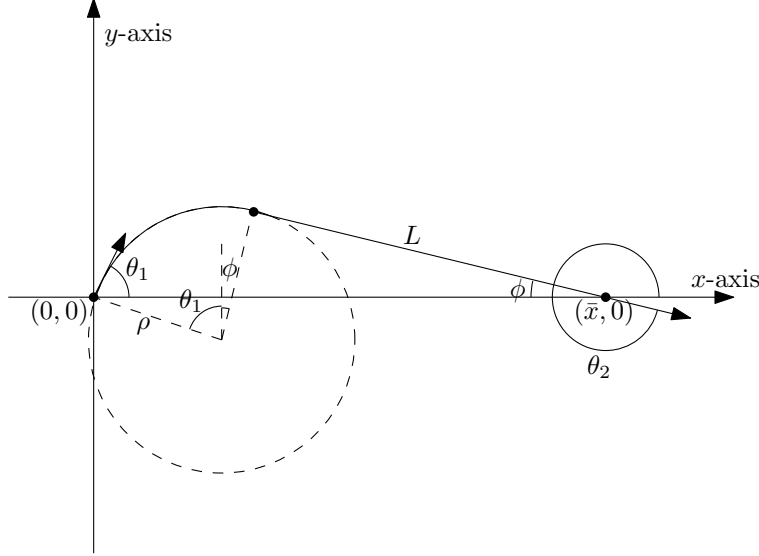


Figure 9. *RS path*

outlined in [23] to convert the ATSP into a symmetric TSP. This method converts an asymmetric instance with n nodes into a symmetric instance with $3n$ nodes. We chose this method primarily because unlike other transformations, there is no big- M constant involved, and therefore we did not have any numerical difficulties such as those faced in [16, 19, 20]. For example, the transformed TSP instance with 32 discretizations at each target has 1920 nodes. Each of the transformed TSP instances was solved to optimality using the CONCORDE solver [24]. The improvement of the lower bounds as the number of discretizations or intervals increases is shown in Fig. 11. On average, the improvement of the lower bounds with respect to the optimal ETSP cost for 32 intervals was 22.28%.

A feasible solution was also obtained by discretizing the angles at each target (32 values) and applying the above transformation procedure. The comparison of the cost of the feasible solution with respect to the optimal Euclidean TSP cost and the lower bound (corresponding to 32 intervals at each target) for the 25 instances is shown in Fig. 12. The average deviation of the cost of the feasible solution from its corresponding lower bound is 5.2%, while the average deviation of the cost of the feasible solution from its corresponding ETSP cost is 29.2%. In one of the instances, we found the cost of the feasible solution from its corresponding lower bound improved by approximately 44%. These results show that the proposed approach can be used to obtain tight lower bounds for the DTSP. A feasible DTSP solution and an optimal solution corresponding to the lower bound for an instance are shown in Fig. 13.

6. Conclusion

We provide a systematic procedure to find lower bounds for the DTSP. This article provides a new direction for developing approximation algorithms for the DTSP. Currently, the transformation method increases the size of the one-in-a-set TSP by 2 or 3 times, resulting in a large TSP. Computationally, more efficient tools for directly solving the one-in-a-set TSP will be useful in finding tighter lower and upper bounds for the DTSP. Future work can also address the same problem with multiple vehicles and other precedence constraints.

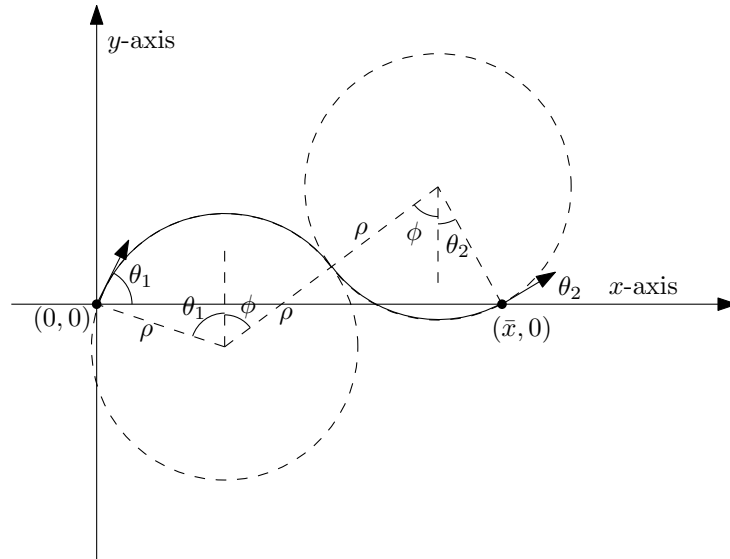


Figure 10. *RL path*

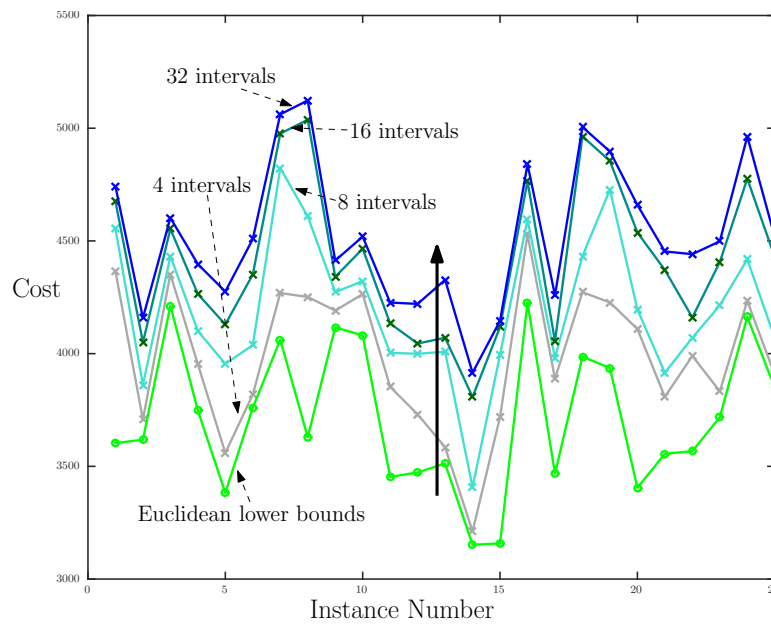


Figure 11. Lower bounds computed with 4, 8, 16, and 32 intervals at each target for 25 instances.

References

- [1] S. Rathinam, R. Sengupta, and S. Darbha, "A resource allocation algorithm for multivehicle systems with nonholonomic constraints," *IEEE Transactions Automation Science and Engineering*, vol. 4, pp. 98–104, 2007.
- [2] J. Le Ny, E. Feron, and E. Frazzoli, "On the dubins traveling salesman problem." *IEEE Trans. Automat. Contr.*, vol. 57, no. 1,

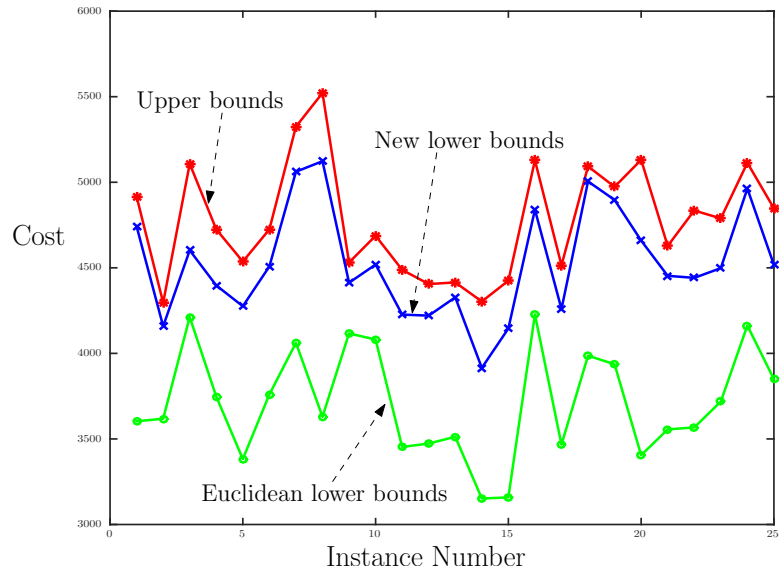


Figure 12. Comparison between lower bounds and upper bounds for 32 discretizations, along with the optimal Euclidean TSP cost.

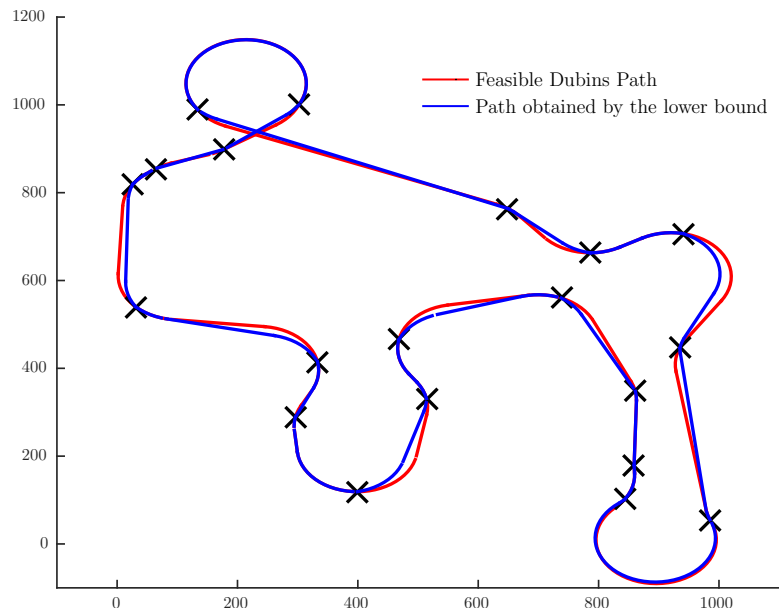
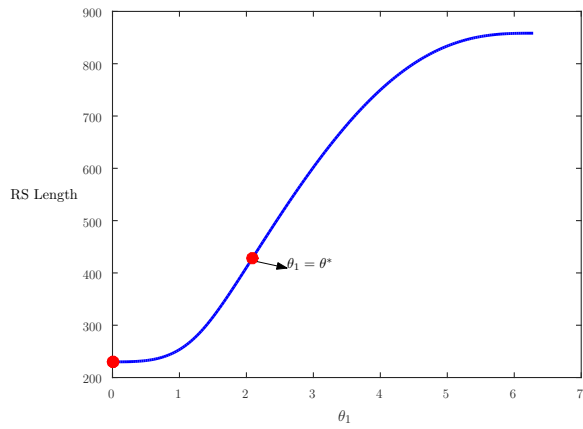


Figure 13. A feasible Dubins path for an instance with 20 targets, and the path obtained from lower bound computation.

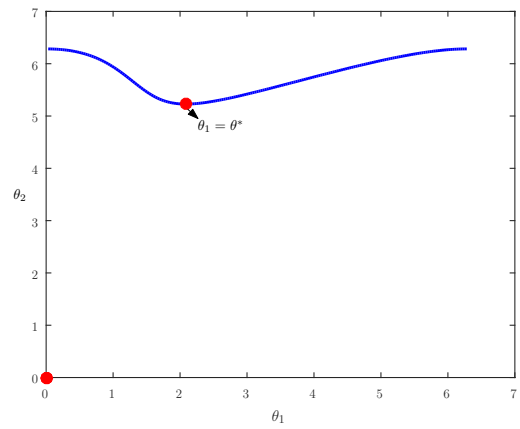
pp. 265–270, 2012.

- [3] P. Chandler and M. Pachter, “Research issues in autonomous control of tactical uavs,” in *American Control Conference, 1998. Proceedings of the 1998*, vol. 1, Jun 1998, pp. 394–398 vol.1.
- [4] A. C. Medeiros and S. Urrutia, “Discrete optimization methods to determine trajectories for dubins’ vehicles,” *Electronic Notes in Discrete Mathematics*, vol. 36, pp. 17 – 24, 2010, {ISCO} 2010 - International Symposium on Combinatorial

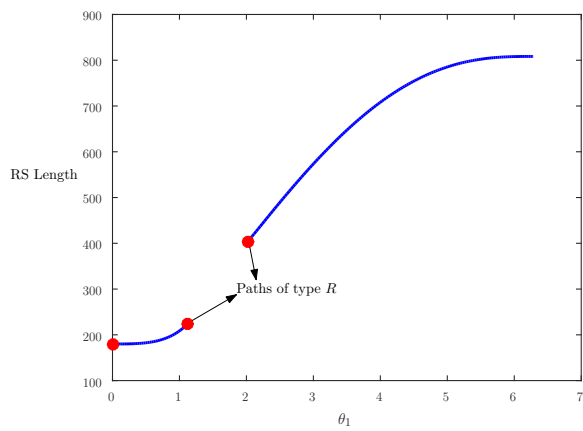
- Optimization. [Online]. Available: <http://www.sciencedirect.com/science/article/pii/S1571065310000041>
- [5] D. Macharet and M. Campos, "An orientation assignment heuristic to the dubins traveling salesman problem," in *Advances in Artificial Intelligence – IBERAMIA 2014*, ser. Lecture Notes in Computer Science, A. L. Bazzan and K. Pichara, Eds. Springer International Publishing, 2014, vol. 8864, pp. 457–468.
 - [6] D. G. Macharet, A. Alves Neto, V. F. da Camara Neto, and M. F. Campos, "Efficient target visiting path planning for multiple vehicles with bounded curvature," in *Intelligent Robots and Systems (IROS), 2013 IEEE/RSJ International Conference on*. IEEE, 2013, pp. 3830–3836.
 - [7] D. G. Macharet, A. A. Neto, V. F. da Camara Neto, and M. F. Campos, "Data gathering tour optimization for dubins' vehicles," in *Evolutionary Computation (CEC), 2012 IEEE Congress on*. IEEE, 2012, pp. 1–8.
 - [8] P. Sujit, B. Hudzietz, and S. Saripalli, "Route planning for angle constrained terrain mapping using an unmanned aerial vehicle," *Journal of Intelligent & Robotic Systems*, vol. 69, no. 1-4, pp. 273–283, 2013.
 - [9] R. J. Kenefic, "Finding good dubins tours for uavs using particle swarm optimization," *Journal of Aerospace Computing, Information, and Communication*, vol. 5, no. 2, pp. 47–56, 2008.
 - [10] D. G. Macharet, A. A. Neto, V. F. da Camara Neto, and M. F. Campos, "Nonholonomic path planning optimization for dubins' vehicles," in *Robotics and Automation (ICRA), 2011 IEEE International Conference on*. IEEE, 2011, pp. 4208–4213.
 - [11] Z. Tang and U. Ozguner, "Motion planning for multitarget surveillance with mobile sensor agents," *Robotics, IEEE Transactions on*, vol. 21, no. 5, pp. 898–908, Oct 2005.
 - [12] K. Savla, E. Frazzoli, and F. Bullo, "Traveling salesperson problems for the dubins vehicle," *IEEE Transactions on Automatic Control*, vol. 53, pp. 1378–1391, 2008.
 - [13] C. Epstein, I. Cohen, and T. Shima, "On the discretized dubins traveling salesman problem," *Technical Report*, 2014.
 - [14] X. Ma, D. Castañón, *et al.*, "Receding horizon planning for dubins traveling salesman problems," in *Decision and Control, 2006 45th IEEE Conference on*. IEEE, 2006, pp. 5453–5458.
 - [15] P. Isaiah and T. Shima, "Motion planning algorithms for the dubins travelling salesperson problem," *Automatica*, vol. 53, pp. 247–255, 2015.
 - [16] P. Oberlin, S. Rathinam, and S. Darbha, "Today's traveling salesman problem," *IEEE Robotics and Automation Magazine*, vol. 17, no. 4, pp. 70–77, Dec. 2010.
 - [17] S. G. Manyam, S. Rathinam, S. Darbha, and K. J. Obermeyer, "Lower bounds for a vehicle routing problem with motion constraints," *International Journal of Robotics and Automation*, vol. 30, no. 3, 2015.
 - [18] S. G. Manyam, S. Rathinam, and S. Darbha, "Computation of lower bounds for a multiple depot, multiple vehicle routing problem with motion constraints," *Journal of Dynamic Systems, Measurement, and Control*, vol. 137, no. 9, p. 094501, 2015.
 - [19] S. G. Manyam, S. Rathinam, S. Darbha, and K. J. Obermeyer, "Computation of a lower bound for a vehicle routing problem with motion constraints," in *ASME 2012 5th Annual Dynamic Systems and Control Conference joint with the JSME 2012 11th Motion and Vibration Conference*. American Society of Mechanical Engineers, 2012, pp. 695–701.
 - [20] S. G. Manyam, S. Rathinam, and S. Darbha, "Computation of lower bounds for a multiple depot, multiple vehicle routing problem with motion constraints," in *Decision and Control (CDC), 2013 IEEE 52nd Annual Conference on*. IEEE, 2013, pp. 2378–2383.
 - [21] S. Manyam, S. Rathinam, D. Casbeer, and E. Garcia, "Shortest paths of bounded curvature for the dubins interval problem," *arXiv preprint arXiv:1507.06980*, 2015.
 - [22] C. E. Noon and J. C. Bean, "A lagrangian based approach for the asymmetric generalized traveling salesman problem," *Operations Research*, vol. 39, no. 4, pp. 623–632, July 1991. [Online]. Available: <http://or.journal.informs.org/content/39/4/623>
 - [23] G. Gutin and A. P. Punnen, Eds., *The traveling salesman problem and its variations*, ser. Combinatorial optimization. Dordrecht, London: Kluwer Academic, 2002. [Online]. Available: <http://opac.inria.fr/record=b1120710>
 - [24] D. L. Applegate, R. E. Bixby, V. Chvatal, and W. J. Cook, *The Traveling Salesman Problem: A Computational Study (Princeton Series in Applied Mathematics)*. Princeton, NJ, USA: Princeton University Press, 2007.
 - [25] L.E. Dubins, "On curves of minimal length with a constraint on average curvature, and with prescribed initial and terminal positions and tangents," *American Journal of Mathematics*, vol. 79, no. 3, pp. 487–516, 1957.
 - [26] X. Goao, H.-S. Kim, and S. Lazard, "Bounded-curvature shortest paths through a sequence of points using convex optimization," *SIAM Journal on Computing*, vol. 42, no. 2, pp. 662–684, 2013. [Online]. Available: <http://dx.doi.org/10.1137/100816079>
 - [27] J.-D. Boissonnat, A. Crzo, and J. Leblond, "Shortest paths of bounded curvature in the plane," *Journal of Intelligent and Robotic Systems*, vol. 11, no. 1-2, pp. 5–20, 1994. [Online]. Available: <http://dx.doi.org/10.1007/BF01258291>



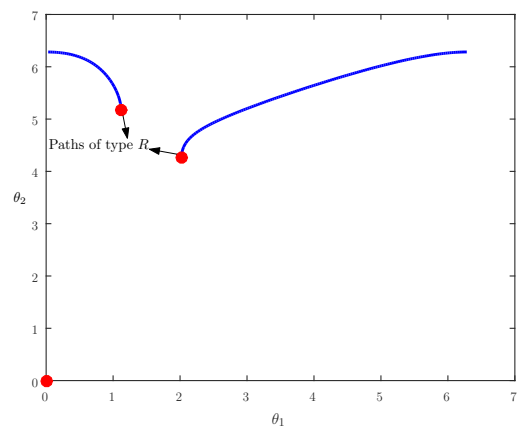
(a) $\bar{x} > 2\rho$



(b) $\bar{x} > 2\rho$



(c) $\bar{x} \leq 2\rho$



(d) $\bar{x} \leq 2\rho$

Figure 14. RS path: examples illustrating $\mathcal{D}(\theta_1)$ and $\theta_2(RS, \theta_1)$.

7. Appendix

7.1. Proof of Lemma 4.1

Using Fig. 9, one can relate L and ϕ to θ_1 using the following equations:

$$\begin{aligned}\rho \sin \phi + L \cos \phi &= \bar{x} - \rho \sin \theta_1, \\ \rho \cos \phi - L \sin \phi &= \rho \cos \theta_1.\end{aligned}\tag{20}$$

The arrival angle $\theta_2(RS, \theta_1)$ at target 2 is equal to $2\pi - \phi$. We now consider two different cases: $\bar{x} > 2\rho$ and $\bar{x} \leq 2\rho$ (the RS path does not exist for a subset of angles of θ_1 if $\bar{x} < 2\rho$).

Case 1: $\bar{x} > 2\rho$.

The length of the RS path is $\mathfrak{D} := (\theta_1 + \phi)\rho + L$. Therefore, $\frac{d\mathfrak{D}}{d\theta_1} := (1 + \frac{d\phi}{d\theta_1})\rho + \frac{dL}{d\theta_1}$. The derivatives of ϕ and L with respect to θ_1 can be obtained by differentiating (20) as follows:

$$(\rho \cos \phi - L \sin \phi) \frac{d\phi}{d\theta_1} + \cos \phi \frac{dL}{d\theta_1} = -\rho \cos \theta_1,\tag{21}$$

$$-(\rho \sin \phi + L \cos \phi) \frac{d\phi}{d\theta_1} - \sin \phi \frac{dL}{d\theta_1} = -\rho \sin \theta_1.\tag{22}$$

Solving these equations and simplifying further, we obtain the following:

$$\frac{d\phi}{d\theta_1} = \frac{\bar{x}}{L} \cos \phi - 1,\tag{23}$$

$$\frac{dL}{d\theta_1} = -\frac{\rho \bar{x}}{L} \cos \theta_1.\tag{24}$$

Therefore,

$$\frac{d\mathfrak{D}}{d\theta_1} = (1 + \frac{d\phi}{d\theta_1})\rho + \frac{dL}{d\theta_1}\tag{25}$$

$$= \frac{\bar{x}}{L}(\rho \cos \phi - \rho \cos \theta_1)\tag{26}$$

$$= \bar{x} \sin \phi.\tag{27}$$

For any $\theta_1 \in [0, 2\pi]$, it is easy to verify geometrically that $\phi \in [0, \pi]$ using Fig. 9. Therefore, $\forall \theta_1 \in (0, 2\pi)$, $\frac{d\mathfrak{D}}{d\theta_1} > 0$, i.e., the length of the RS path increases monotonically from \bar{x} . When $\theta_1 = 2\pi$, the curved segment in the RS path vanishes and the length of the RS path returns to the Euclidean distance between the targets (\bar{x}). Even though the length of the RS path increases monotonically for any $\theta_1 \in [0, 2\pi)$, the arrival angle at target 2, $\theta_2 := 2\pi - \phi$, first decreases with θ_1 , reaches a minimum at some $\theta_1 = \theta^*$, and increases to 2π . This minimum can be computed by solving $\frac{d\phi}{d\theta_1} = 0 \Rightarrow \frac{\bar{x}}{L} \cos(\phi(\theta^*)) - 1 = 0$ or $\cos(\phi(\theta^*)) = \frac{L}{\bar{x}}$. One can verify that at $\theta_1 = \theta^*$, θ_2 reaches a minimum.

Now, the optimum for $\min_{\theta_1 \in I_1} \{RS^1(\theta_1)\}$ must satisfy one of the following conditions:

1. $\frac{d\mathfrak{D}}{d\theta_1} = 0$ or $\theta_1 = 0$ ($\frac{d\mathfrak{D}}{d\theta_1}$ does not exist at this point) or $\theta_1 = \theta_1^{min}$ or $\theta_1 = \theta_1^{max}$. $\forall \theta_1 \in (0, 2\pi)$, $\frac{d\mathfrak{D}}{d\theta_1} \neq 0$. As the length of the RS path increases monotonically with respect to θ_1 , we need not consider $\theta_1 = \theta_1^{max}$. Therefore, for this condition, the optimum occurs when $\theta_1 = 0$ or $\theta_1 = \theta_1^{min}$.

2. $\theta_2 = \theta_2^{min}$ or $\theta_2 = \theta_2^{max}$.

Therefore, when $\bar{x} > 2\rho$, $\min_{\theta_1 \in I_1} \{RS^1(\theta_1)\} := \min\{d_S, RS^1(\theta_1^{min}), RS^2(\theta_2^{min}), RS^2(\theta_2^{max})\}$.

Case 2: $\bar{x} \leq 2\rho$.

In this case, the RS path is not defined for any $\theta_1 \in (\sin(\frac{\bar{x}}{2\rho}), \frac{\pi}{2} + \cos(\frac{\bar{x}}{2\rho}))$. Moreover, when $\theta_1 = \sin(\frac{\bar{x}}{2\rho})$ or $\theta_1 = \frac{\pi}{2} + \cos(\frac{\bar{x}}{2\rho})$, the RS path reduces to just one segment of type R . Therefore, following the same analysis as in the previous case, $\min_{\theta_1 \in I_1} \{RS^1(\theta_1)\} := \min\{d_S, d_R, RS^1(\theta_1^{min}), RS^2(\theta_2^{min}), RS^2(\theta_2^{max})\}$. Hence this case is proved.

7.2. Proof of Lemma 4.2

We can solve for ϕ and θ_2 using the following equations (Fig. 10):

$$\begin{aligned} 2\rho \cos \phi - \rho \cos \theta_2 &= \rho \cos \theta_1, \\ 2\rho \sin \phi + \rho \sin \theta_2 &= \bar{x} - \rho \sin \theta_1. \end{aligned} \quad (28)$$

Differentiating and simplifying these equations, we get

$$-2 \sin \phi \frac{d\phi}{d\theta_1} + \sin \theta_2 \frac{d\theta_2}{d\theta_1} = -\sin \theta_1, \quad (29)$$

$$2 \cos \phi \frac{d\phi}{d\theta_1} + \cos \theta_2 \frac{d\theta_2}{d\theta_1} = -\cos \theta_1. \quad (30)$$

Solving further for $\frac{d\phi}{d\theta_1}$ and $\frac{d\theta_2}{d\theta_1}$, we get

$$\frac{d\phi}{d\theta_1} = \frac{\sin(\theta_1 - \theta_2)}{2 \sin(\phi + \theta_2)}, \quad (31)$$

$$\frac{d\theta_2}{d\theta_1} = -\frac{\sin(\theta_1 + \phi)}{\sin(\phi + \theta_2)}, \quad (32)$$

$$\begin{aligned} \frac{d\mathcal{D}}{d\theta_1} &= \rho \left(1 + \frac{d\theta_2}{d\theta_1} + 2 \frac{d\phi}{d\theta_1} \right) \\ &= \rho \left(1 - \frac{\sin(\theta_1 + \phi)}{\sin(\phi + \theta_2)} + \frac{\sin(\theta_1 - \theta_2)}{\sin(\phi + \theta_2)} \right). \end{aligned} \quad (33)$$

Equating $\frac{d\mathcal{D}}{d\theta_1} = 0$ and simplifying the equations, we get either $\phi + \theta_1 = 0$ or $\phi + \theta_2 = 0$ or $\theta_1 = \theta_2$. $\phi + \theta_1 = 0$ or $\phi + \theta_2 = 0$ would imply that one of the circles vanishes; however, this is possible only when $\bar{x} \leq 2\rho$. When $\theta_1 = \theta_2$, we note that $\frac{d\theta_2}{d\theta_1} = -1$ and $\frac{d\phi}{d\theta_1} = 0$. Using this, one can verify that $\frac{d^2\mathcal{D}}{d\theta_1^2} = \frac{2(1 - \cos(\theta_1 + \phi))}{\sin(\theta_1 + \phi)} \Rightarrow \frac{d^2\mathcal{D}}{d\theta_1^2} > 0$. Therefore, the length of the RL path reaches a minimum when $\theta_1 = \theta_2$.

Case 1: $4\rho \geq \bar{x} \geq 2\rho$.

The optimum for $\min_{\theta_1 \in I_1} \{RL^1(\theta_1)\}$ must occur at one of the extreme values of $\mathcal{D}(\theta_1)$ or when $\theta_1 \in \{\theta_1^{min}, \theta_1^{max}\}$ or $\theta_2 \in \{\theta_2^{min}, \theta_2^{max}\}$. $\mathcal{D}(\theta_1)$ reaches a local minimum at $\theta_1 = \theta_1^*$ (Fig. 15). Also, the RL path just ceases to exist when $\theta_1 = \theta_1^{2*}$ or $\theta_1 = \theta_1^{3*}$. Specifically, for a small $\varepsilon > 0$, the RL path does not exist when

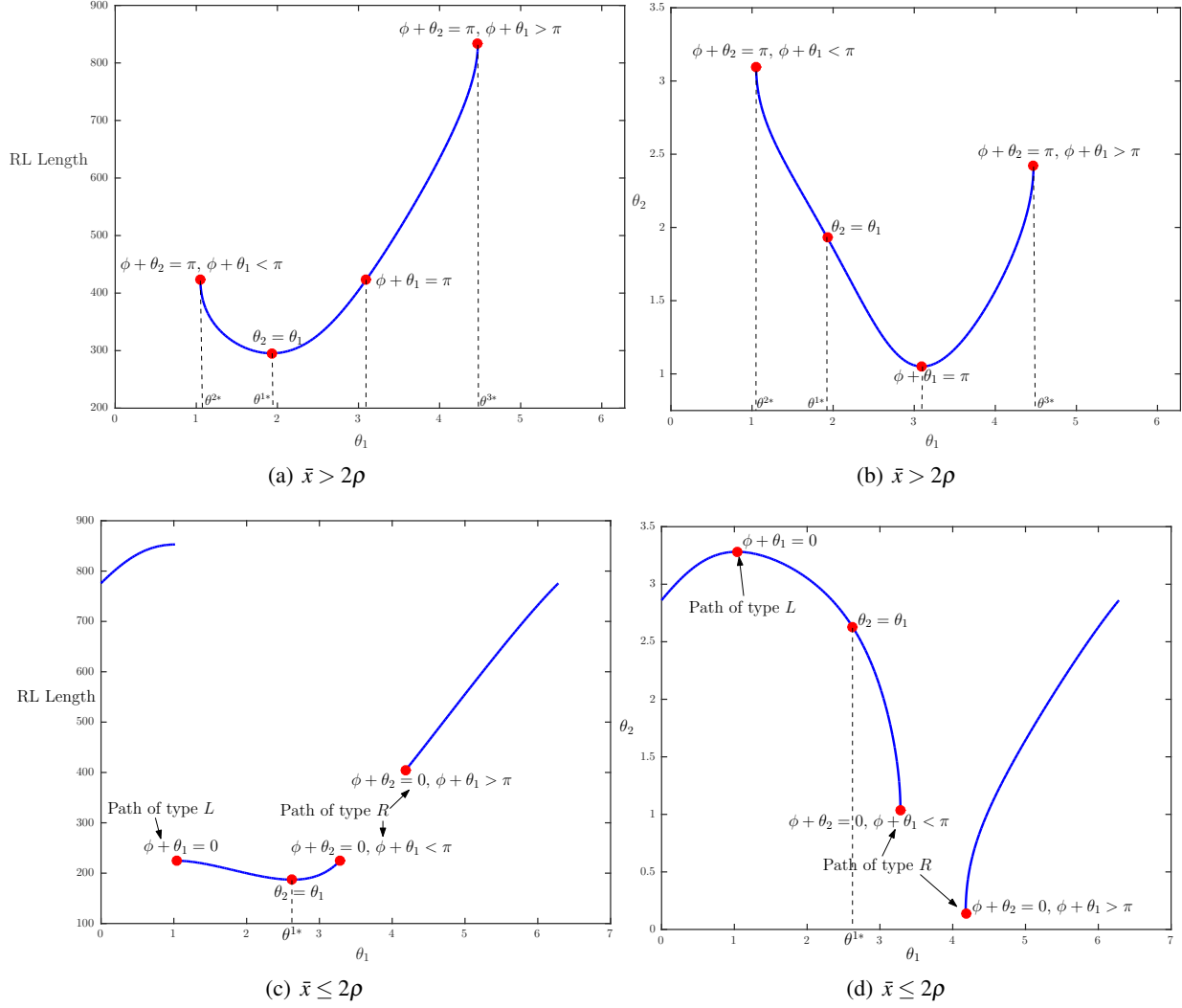


Figure 15. *RL Path*: examples illustrating $\mathcal{D}(\theta_1)$ and $\theta_2(RL, \theta_1)$ for the case when $0 \leq \phi + \theta_2 \leq \pi$.

$\theta_1 = \theta^{2*} - \varepsilon$ or $\theta_1 = \theta^{3*} + \varepsilon$. Therefore, $\min_{\theta_1 \in I_1} \{RL^1(\theta_1)\} := \min\{RL^1(\theta^{1*}), RL^1(\theta^{2*}), RL^1(\theta^{3*}), RL^*\}$.

Case 2: $2\rho \geq \bar{x} \geq 0$.

In this case, one of the circles may cease to exist, and therefore the optimum may be equal to d_L or d_R if the corresponding angle constraints are met. Following the same arguments as in the previous case, we obtain $\min_{\theta_1 \in I_1} \{RL^1(\theta_1)\} := \min\{d_L, d_R, RL^1(\theta^{1*}), RL^*\}$. Hence this case is proved.